EUROPEAN ORGANIZATION FOR NUCLEAR RESEARCH

CERN/PPE 93-133
28 July 1993

First results from experiment WA91 at the CERN Omega Spectrometer

The WA91 Collaboration

F. Antinori[4], D. Barberis[4], R.P. Barnes[3], A. Bayes[3], W. Beusch[4], J.N. Carney[3], S. Clewer[3], J.P. Davies[3], D. Di Bari[2], C.J. Dodenhoff[3], D. Evans[4], R. Fini[2], B.R. French[4], B. Ghidini[2], M. Girone[2], A. Jacholkowski[2], J.B. Kinson[3], A. Kirk[4], V. Lenti[2], A. Loconsole[2], S. Maljukov[5], V. Manzari[2], I. Minashvili[5], F. Navach[2], E. Quercigh[4], V. Romanovsky[5], N. Russakovich[5], A. Semenov[5], M. Sené[4], R. Sené[4], A. Solovjev[5], G. Tchlatchidze[5], G. Vassiliadis[1], I. Vichou[1], O. Villalobos Baillie[3], M.F. Votruba[3]

Presented by: A. Kirk, CERN at Hadron 93, Como, Italy, June 1993

1 Athens University, Nuclear Physics Department, Athens, Greece.
2 Dipartimento di Fisica dell'Università and Sezione INFN, Bari, Italy.
3 University of Birmingham, Physics Department, Birmingham, U.K.
4 CERN, European Organization for Nuclear Research, Geneva, Switzerland.
5 JINR, Dubna, Russia.

Abstract

Experiment WA91 searches for non-$q\bar{q}$ mesons produced in the central region in the reaction $pp \rightarrow p_f(X^0)p_s$ at 450 GeV/c using the CERN Omega Spectrometer. WA91 is a continuation of the WA76 experiment which has studied this reaction using beams of 85 and 300 GeV/c. Preliminary results from experiment WA91 are presented. In Particular the X(1450) and X(1900) observed for the first time in the $\pi^+\pi^-\pi^+\pi^-$ channel of the WA76 experiment at 300 GeV/c are confirmed by the WA91 data.

1 Introduction

Experiment WA91 uses the CERN Omega Spectrometer to search for non-$q\bar{q}$ mesons produced in the central region in the reaction $pp \rightarrow p_f(X^0)p_s$ at 450 GeV/c, where the subscripts f and s indicate the fastest and slowest particles in the laboratory respectively. The reaction is isolated firstly at the trigger level by the selection of a fast and slow particle (as described below) and secondly, at the analysis stage, by the requirement of transverse and longitudinal momentum balance between the incident and outgoing particles.

The experiment was motivated by the interesting signals observed by the WA76 experiment in central production at 85 and 300 GeV/c [1]. This paper present the first results from experiment WA91 on 40 % of the statistics recorded during its 1992 data taking.

2 Experimental layout and trigger

The layout of the Omega Spectrometer used in the WA91 experiment is shown in fig. 1 and comprises:

1. A set of detectors to perform an accurate measurement of the incident beam direction. This was achieved by using a telescope of ten 20 μm pitch microstrip detectors (5y and 5z planes).

2. A 60 cm long hydrogen target and a system of scintillator hodoscopes for the trigger definition (as described below).

3. Fifteen 2mm pitch (A and B) Multi-Wire Proportional Chambers (MWPC), one 1mm pitch MWPC and two Drift Chambers (DC) to measure the medium momentum charge tracks.

4. Sixteen 2mm pitch (C) MWPCs to measure the slow proton.

5. A system of microstrip detectors (see fig.2(a)) placed just after the target and in 3 stations 5, 10 and 12 m downstream of the centre of Omega in order to measure the outgoing fast track which was typically in the momentum range 350-450 GeV/c.

6. The Olga Lead glass calorimeter used for the measurement of γ s.

The trigger of the experiment required:

1. A fast particle crossing the downstream microstrip telescope. This requirement was fulfilled by asking for a coincidence between two scintillation counters (A1 and A2) placed close to the microstrip detectors at 5 and 10 m.

2. A slow particle left [right] was defined by requiring one hit on any of the fourteen slabs of the Slow Proton Counter Left (SPC(L)) [Right (SPC(R))] in coincidence with a hit in the left [right] box counter (TB) and $\geq$ 1 hit in 2 planes of the C MWPCs on the left [right] side of the target.

3. In order to reduce backward diffraction or excitation events no hit was required in the other three sides of the box counter (TB) which was left open at its front end to allow particles produced centrally to escape downstream.

Elastic scattering events are automatically rejected when the slow proton and fast proton are on the same side i.e. a slow proton left and a hit in the A2(L) counter or a slow proton right together with a hit in A2(R). However the other combinations are dominated by elastic scattering. Therefore for the combinations slow proton left and A2(R) or slow proton right and A2(L) we reduce the number of elastic scattering events triggered on by asking that either energy is seen in the calorimeter or that there are 2 or more hits in an A MWPC outside the fast track region.

The alignment of the microstrip system which is critical for the isolation of momentum balancing events has been performed on a run by run basis using beam triggers which were taken interleaved with the physics triggers. The results of the alignment procedure is summarised in fig. 2(b) where the reconstructed beam distribution can be seen to have $\sigma = 2.0$ GeV/c.

3 Selection of the reaction $pp \rightarrow p_f(\pi^+\pi^-)p_s$

The reaction $pp \rightarrow p_f(\pi^+\pi^-)p_s$ has been isolated from the sample of events having four outgoing tracks by first imposing cuts on the components of missing momentum ($|missingP_z| < 0.08$ GeV/c, $|missingP_y| < 0.16$ GeV/c and $|missingP_x| < 14$ GeV/c). Fig. 3(a) shows the total missing transverse momentum between the incident beam and outgoing particles. The distribution shows a narrow peak at threshold indicating the presence of "4C" events. Fig. 3(b) shows the resulting longitudinal missing momentum distribution, after placing a cut on the missing P_T, which has a peak centered at zero with very little background. These plot show that momentum balance events can be isolated and hence that exclusive channels can be studied.

Fig. 4(a) shows the Feynman x distribution for the slow proton, the $\pi^+\pi^-$ system and the fast proton respectively. A peak can be seen in the $\pi^+\pi^-$ system near $x_F = 0$ but the distribution also spreads to higher x_F values. Fig. 4(b) shows the effective mass of the fast proton and π^+ where a clear Δ^{++} signal can be seen. To reject events containing a Δ^{++} $m(p_f\pi^+) \geq 1.5$ GeV is required. The x_F distribution for the remaining events is shown in fig. 4(c) where a clear peak corresponding to the centrally produced events can be seen.

The slow particle is identified as a proton by applying a cut to the pulse height in the SPC as a function of momentum. In order to ensure that the central particles are πs the Ehrlich mass squared [2] is plotted in fig. 5(a) for the events passing the above selection cuts. The peak at the π mass squared is the signal of the centrally produced $\pi^+\pi^-$ final state and a shoulder can be seen at the kaon mass squared.

The $\pi^+\pi^-$ channel (245 584 events) has been isolated from the other central two-body final states by requiring the Ehrlich mass squared to be in the range -0.3 to 0.2 GeV^2. The centrally produced $\pi^+\pi^-$ mass spectrum is shown in fig. 5(b). There is a small amount of $\rho(770)$, a sharp drop around $K\overline{K}$ threshold (the so called $S^*/f_0(975)$ region) and some $f_2(1270)$.

To fit the mass spectrum shown in fig. 5(b) we have used the parameterisation described in ref. [3] which uses a coupled channel Breit-Wigner to describe the $S^*/f_0(975)$. The fit probability is 48

% and the parameters of the $S^*/f_0(975)$ are $m_0 = 979 \pm 4$ MeV, $G_\pi = 0.22 \pm 0.04$ and $G_K = 0.69 \pm 0.3$ compatible with those found by WA76 [3].

4 Selection of the reaction $pp \rightarrow p_f(\pi^+\pi^-\pi^+\pi^-)p_s$

The reaction $pp \rightarrow p_f(\pi^+\pi^-\pi^+\pi^-)p_s$ has been isolated from the sample of events having six outgoing tracks by first imposing cuts on the components of missing momentum ($|missingP_z| < 0.08$ GeV/c, $|missingP_y| < 0.12$ GeV/c and $|missingP_x| < 14$ GeV/c). The slow particle is identified as a proton by applying a cut to the pulse height in the SPC as a function of momentum. The Delta function defined as :

$$\Delta = MM^2(p_f p_s) - M^2(\pi^+\pi^-\pi^+\pi^-)$$

is then calculated for each event and a cut of $|\Delta| \leq 3.0$ (GeV)^2 is used to select the $\pi^+\pi^-\pi^+\pi^-$ channel. Events containing a fast Δ^{++} are again removed leaving 55908 centrally produced $\pi^+\pi^-\pi^+\pi^-$ events. The mass spectrum of these events are shown in fig. 6(a) where in addition to the clear peak at 1.28 GeV, due to the $f_1(1285)$, there are also enhancements at 1.45 and 1.9 GeV, referred to as the X(1450) and X(1900). In addition there are reflections from the $\eta\pi^+\pi^-$ decay of the η' and $f_1(1285)$ which give small enhancements in the $\pi^+\pi^-\pi^+\pi^-$ mass spectrum in the 0.8 and 1.1 GeV regions due to a slow π^0 from the decay of an η falling within the missing momentum cuts.

In order to study further the X(1450) and X(1900) a cut is placed on the variable t defined as $t = |t_1| + |t_2|$, where t_1 and t_2 are the four momentum transfer squared at the slow and fast vertices respectively. Fig. 6(b) and (c) show the $\pi^+\pi^-\pi^+\pi^-$ mass spectrum for $t < 0.3$ GeV^2 and $t > 0.3$ GeV^2 respectively. The $f_1(1285)$ is clearly visible in both spectra whilst the X(1450) and X(1900) are produced predominantly at low t.

Fig. 6(a) and (b) have been fitted using Breit-Wigners to describe the $f_1(1285)$, X(1450) and X(1900) together with histograms to describe the η' and $f_1(1285)$ reflections and a background of the form $(m - m_{th})^a exp(-bm - cm^2)$, where m is the $\pi^+\pi^-\pi^+\pi^-$ mass, m_{th} is the $\pi^+\pi^-\pi^+\pi^-$ threshold mass and a, b and c are fit parameters. The fit gives

$f_1(1285)$	M = 1280 ± 2	MeV	Γ = 40 ± 6	MeV
X(1450)	M = 1444 ± 4	MeV	Γ = 50 ± 16	MeV
X(1900)	M = 1934 ± 15	MeV	Γ = 350 ± 75	MeV

compatible with those values found in the WA76 experiment at 300 GeV/c [4] and hence the results from WA91 confirm the existence of the X(1450) and X(1900).

5 Preliminary results from the Gamma calorimeter

The gamma calorimeter data has been passed through a preliminary version of the Olga reconstruction code. Showers in Olga associated with charged track impacts have been removed.

The reaction $pp \rightarrow p_f(\pi^+\pi^-\gamma\gamma)p_s$ has been isolated from the sample of events having four outgoing charged tracks plus two γs with energy greater than 1 GeV deposited in Olga by first imposing the momentum balance cuts described above. The effective mass of the two γs is shown in fig. 7(a) where a clear π^0 can be seen (σ = 20 MeV) which is selected by requiring $0.1 < m(\gamma\gamma) < 0.17$ GeV. Increasing the minimum energy of the γs to 2 GeV produces the $\gamma\gamma$ mass spectrum shown in fig. 7(b) where a clear η can be seen (σ = 40 MeV) which is selected by requiring $0.45 < m(\gamma\gamma) < 0.65$ GeV.

The resulting $\pi^+\pi^-\pi^0$ mass spectrum is shown in fig. 7(c) where signals of the η and ω can be seen. Fig 7(d) shows the resulting $\eta\pi^+\pi-$ mass spectrum where peaks can be observed at the η' and $f_1(1285)$ masses.

6 Summary

Preliminary results from experiment WA91 are presented. In Particular the X(1450) and X(1900) observed for the first time in the $\pi^+\pi^-\pi^+\pi^-$ channel of the WA76 experiment at 300 GeV/c are confirmed by the WA91 data.

References

[1] T. A. Armstrong et al., Phys. Lett. **B146** (1984) 273, Phys. Lett **B166** (1986) 245, Phys. Lett **B167** (1986) 133, Zeit. Phys **C34** (1987) 23, Zeit. Phys **C34** (1987) 33, Zeit. Phys **C35** (1987) 167, Nucl. Instr. and Methods **A274** (1989) 165, Zeit. Phys **C43** (1989) 55, Phys. Lett **B221** (1989) 221, Phys. Lett **B221** (1989) 216, Phys. Lett **B227** (1989) 186, Phys. Lett **B228** (1989) 536, Zeit. Phys **C46** (1990) 405, Zeit. Phys **C48** (1990) 213, Zeit. Phys **C51** (1991) 351, Zeit. Phys **C52** (1991) 389.

[2] R. Ehrlich et al., Phys. Rev. Lett. 20 (1968) 686.

[3] T. A. Armstrong et al., Zeit. Phys. **C51** (1991) 351.

[4] T. A. Armstrong et al., Phys. Lett. **B228** (1989) 536.

[5] T. A. Armstrong et al., Zeit. Phys. **C56** (1992) 29.

Figure Captions

Fig. 1 Layout of the CERN Omega Spectrometer for experiment WA91.

Fig. 2 a) Layout of the microstrips used to measure the beam and fast track

b) The reconstructed beam momentum.

Fig. 3 Missing momentum distributions for the four prong events.

a) Missing transverse momentum distribution.

b) Missing longitudinal momentum distribution after a cut on the missing P_T.

Fig. 4 a) Feynman x distribution for the slow proton, the $\pi^+\pi^-$ system and fast proton.

b) The effective mass of the fast proton and π^+.

c) Feynman x distribution after removing events with a fast Δ^{++}.

Fig. 5 a) Ehrlich mass squared distribution.

b) $\pi^+\pi^-$ mass spectrum with fit described in the text.

Fig. 6 $\pi^+\pi^-\pi^+\pi^-$ mass spectrum for a) all t, b) $t < 0.3$ GeV^2 and c) $t > 0.3$ GeV^2.

Fig. 7 a) and b) $\gamma\gamma$ effective mass spectrum.

c) $\pi^+\pi^-\pi^0$ and d) $\pi^+\pi^-\eta$ mass spectra.

Ω LAYOUT FOR WA91 (1992 RUN)

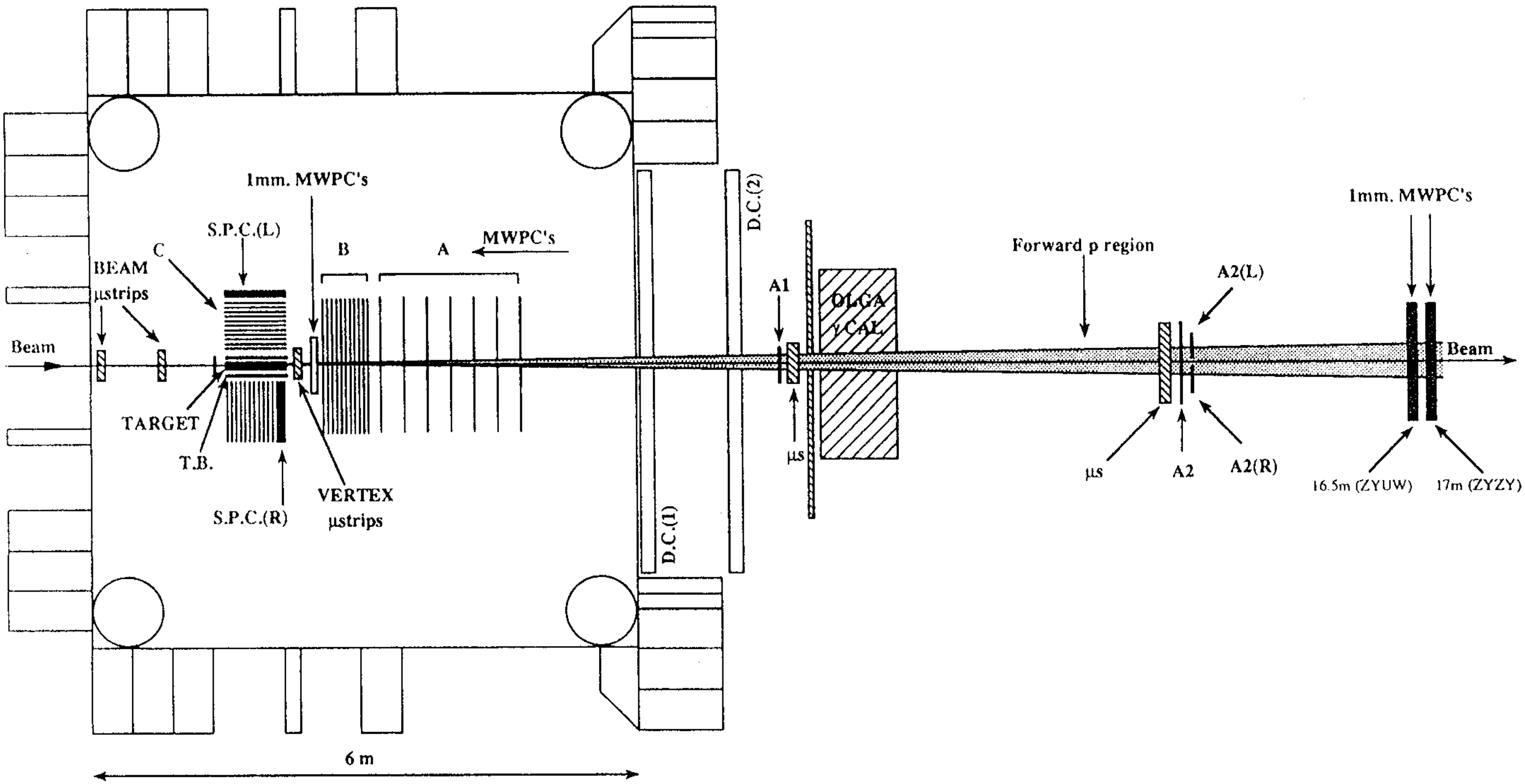

Fig. 1

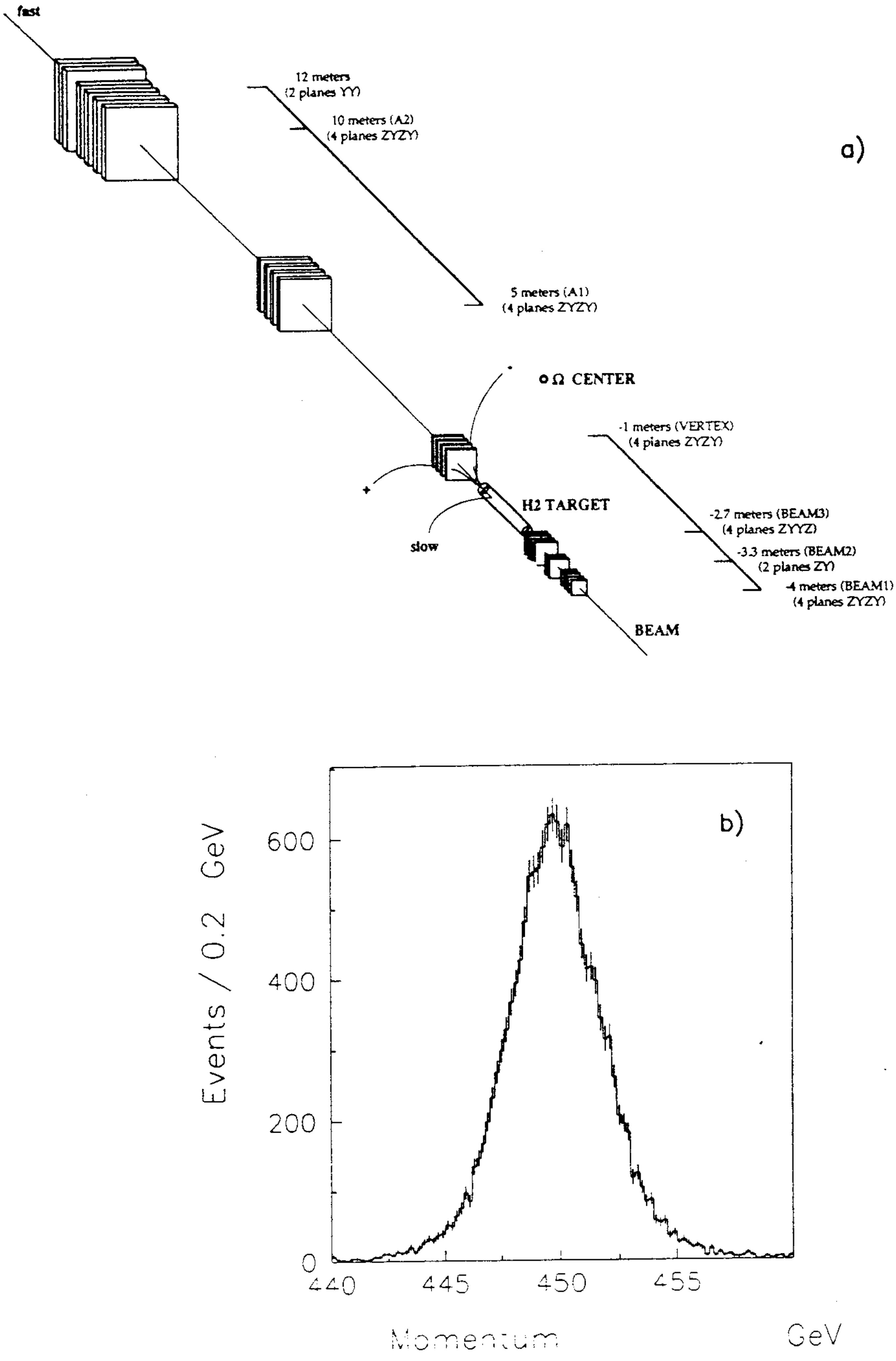
fast
12 meters
(2 planes YY)
10 meters (A2)
(4 planes ZYZY)
a)
5 meters (A1)
(4 planes ZYZY)
Ω CENTER
-1 meters (VERTEX)
(4 planes ZYZY)
H2 TARGET
slow
-2.7 meters (BEAM3)
(4 planes ZYYZ)
-3.3 meters (BEAM2)
(2 planes ZY)
-4 meters (BEAM1)
(4 planes ZYZY)
BEAM
b)
Events / 0.2 GeV
0
200
400
600
440
445
450
455
Momentum
GeV

Fig. 2

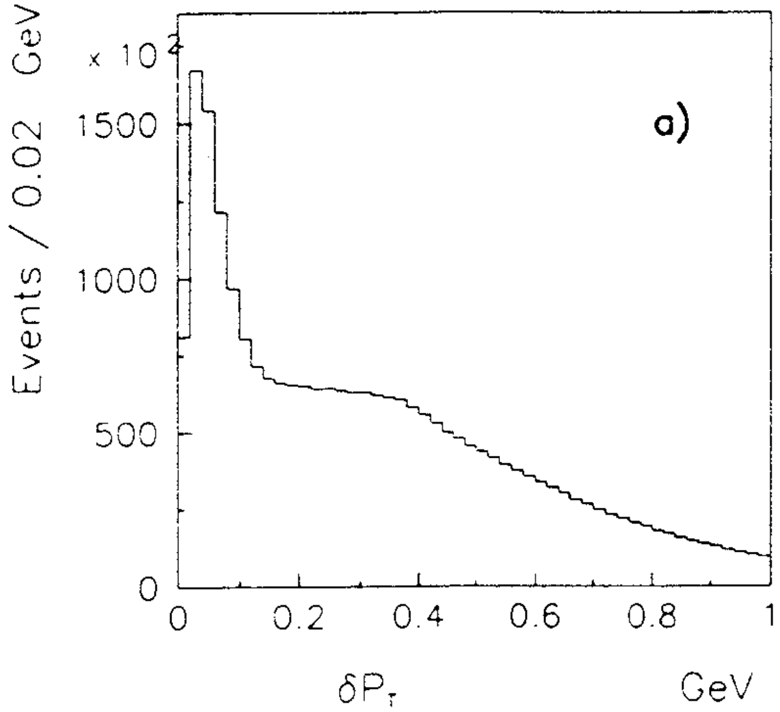

Events / 0.02 GeV
x 10^2
1500
1000
500
0
a)
0
0.2
0.4
0.6
0.8
1
δP_T
GeV

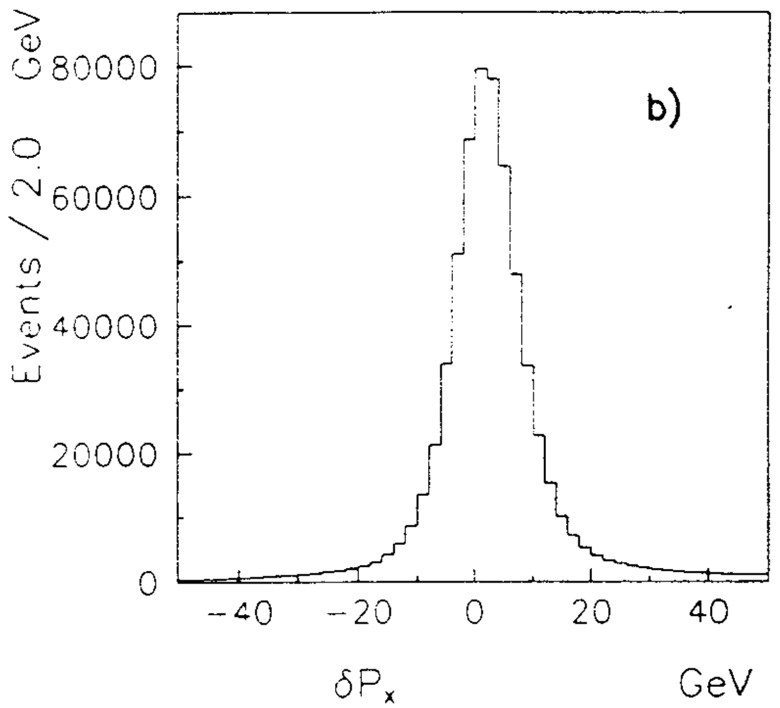

Events / 2.0 GeV
80000
60000
40000
20000
0
b)
-40
-20
0
20
40
δP_x
GeV

Fig. 3

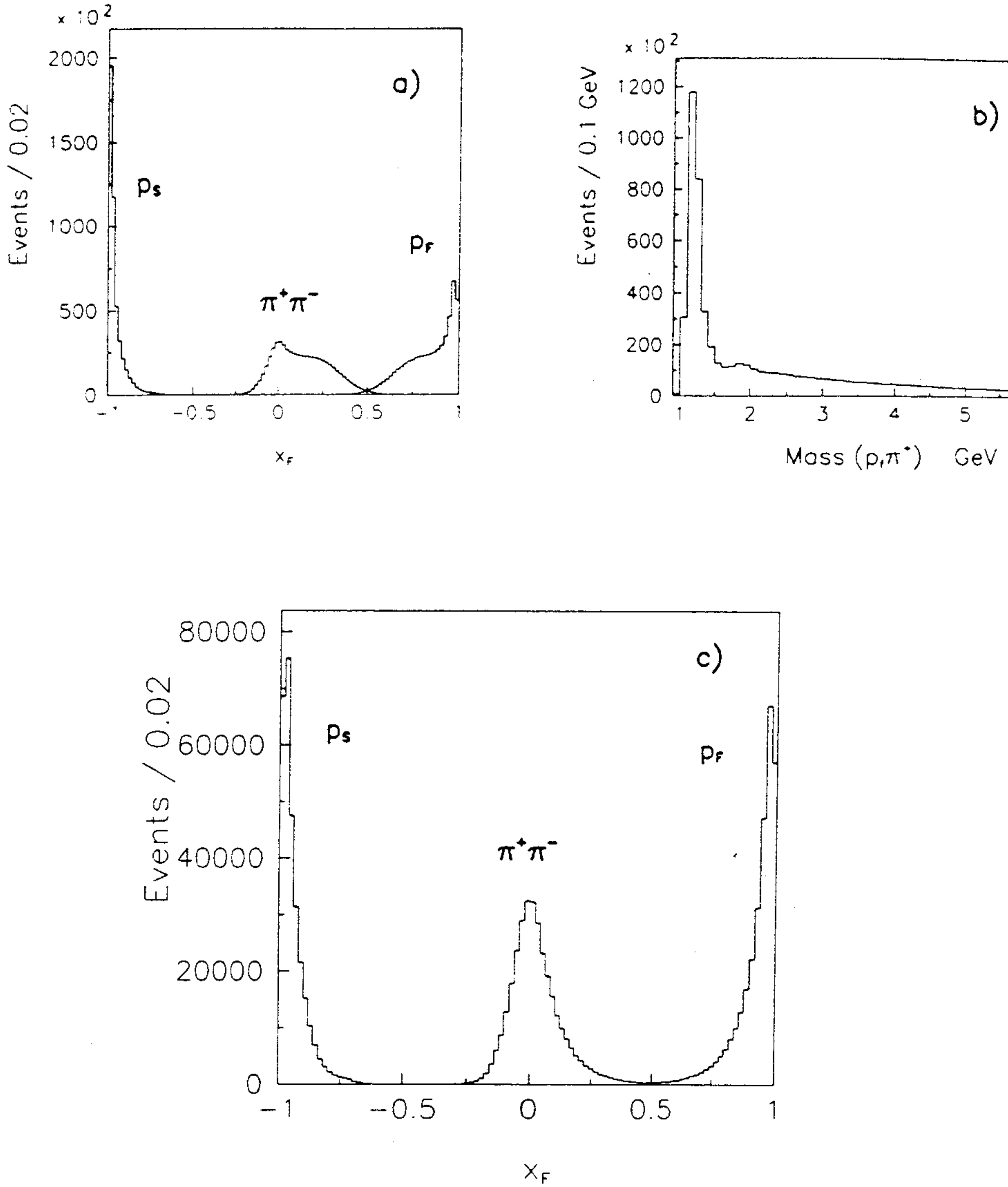

x 10^2
Events / 0.02
2000
1500
1000
500
0
a)
p_s
p_F
π⁺π⁻
-1
-0.5
0
0.5
1
x_F
x 10^2
Events / 0.1 GeV
1200
1000
800
600
400
200
0
b)
1
2
3
4
5
Mass (p,π⁺) GeV
80000
60000
40000
20000
0
Events / 0.02
c)
p_s
p_F
π⁺π⁻
-1
-0.5
0
0.5
1
x_F

Fig. 4

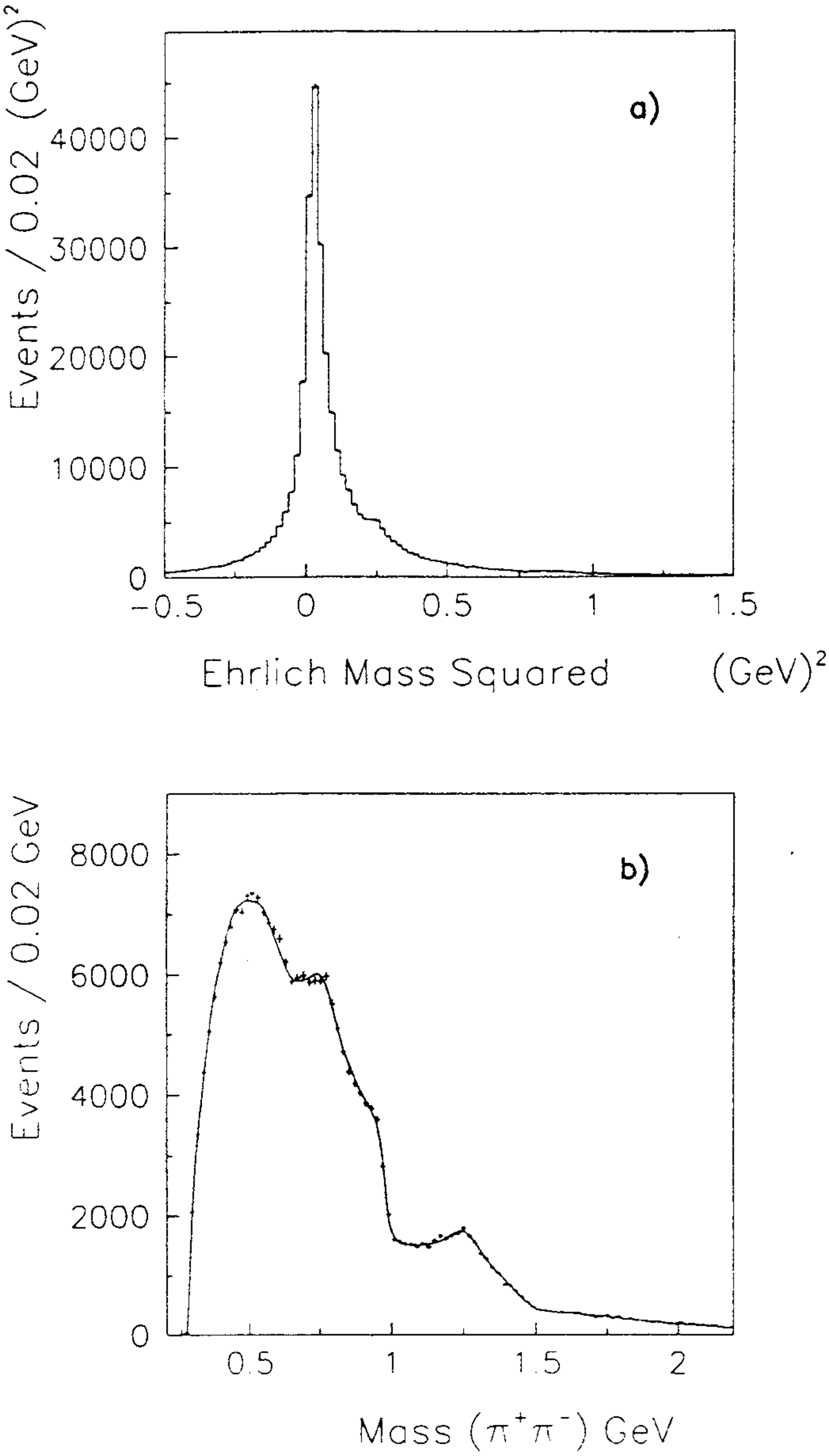
a)
Events / 0.02 (GeV)²
40000
30000
20000
10000
0
−0.5
0
0.5
1
1.5
Ehrlich Mass Squared (GeV)²
b)
Events / 0.02 GeV
8000
6000
4000
2000
0
0.5
1
1.5
2
Mass (π⁺π⁻) GeV

Fig. 5

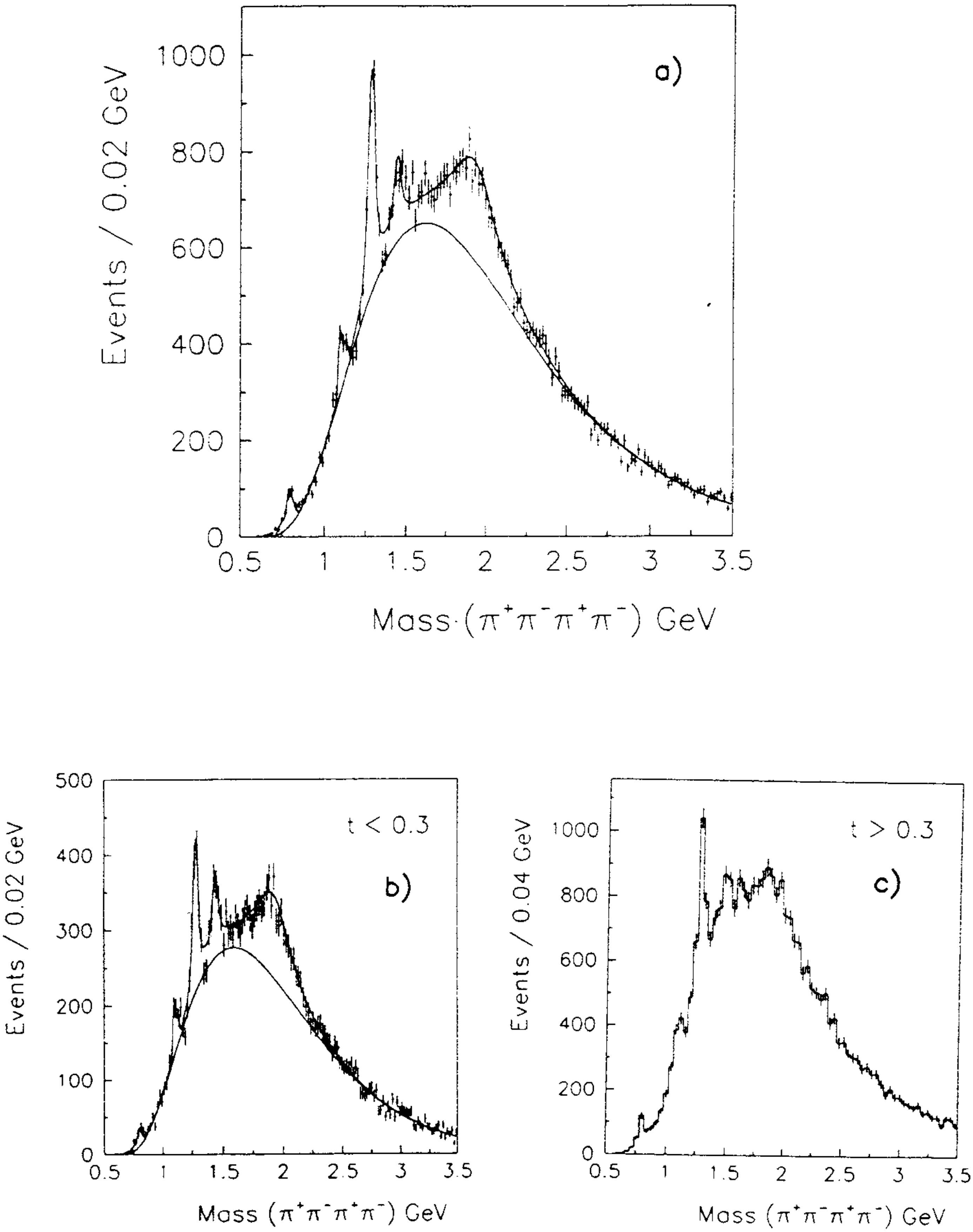
a)
Events / 0.02 GeV
1000
800
600
400
200
0
0.5
1
1.5
2
2.5
3
3.5
Mass $(\pi^+\pi^-\pi^+\pi^-)$ GeV
t < 0.3
b)
Events / 0.02 GeV
500
400
300
200
100
0
Mass $(\pi^+\pi^-\pi^+\pi^-)$ GeV
t > 0.3
c)
Events / 0.04 GeV
1000
800
600
400
200
0
Mass $(\pi^+\pi^-\pi^+\pi^-)$ GeV

Fig. 6

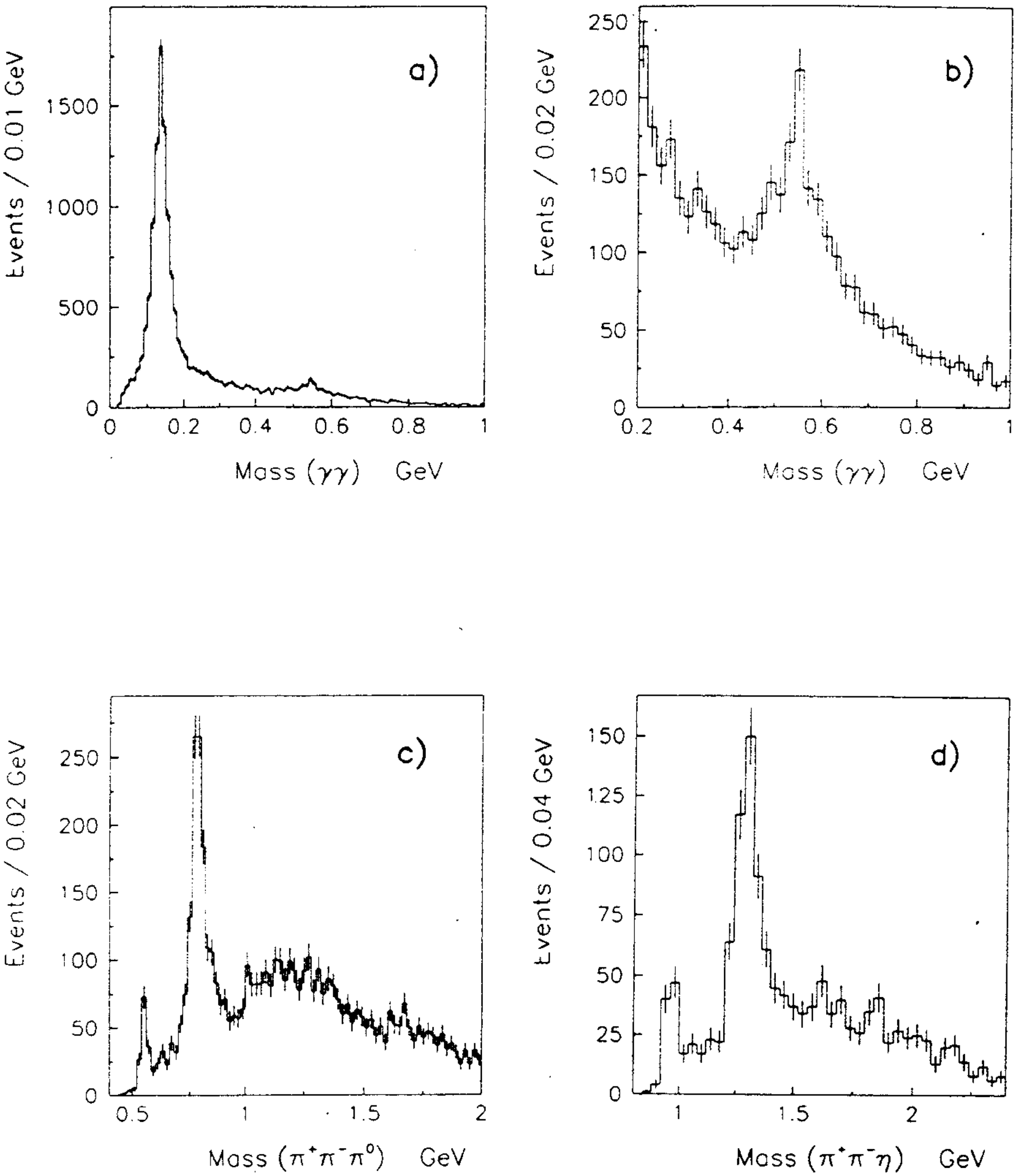
a)
Events / 0.01 GeV
Mass (γγ) GeV
b)
Events / 0.02 GeV
Mass (γγ) GeV
c)
Events / 0.02 GeV
Mass (π⁺π⁻π⁰) GeV
d)
Events / 0.04 GeV
Mass (π⁺π⁻η) GeV

Fig. 7